Journal of Glaciology, Vol. 26, No. 94, 1980

A FRAGMENT-FLOW MODEL OF DRY-SNOW AVALANCHES

By ARTHUR I. MEARS
(222 East Gothic Avenue, Gunnison, Colorado 81230, U.S.A.)

ABSTRACT. Field data on dry-slab avalanches obtained during the period 1975–79 from several snow climates suggest the following: (1) most of the mass of the typical avalanche studied consisted of fragments with lengths greater than 5 cm, (2) transverse and longitudinal shear planes formed during deceleration in the avalanche run-out zone, and (3) the flow height exceeded the slab height in most cases. No correlation was found between the run-out distance and the track or run-out zone slope, or between the run-out distance and the released slab height.

The field data suggest that avalanche motion is best described as a flow of fragments in which boundary shearing stresses are sensitive to fragment size distributions and volumetric solids concentrations. These factors may be more important than the roughness of the avalanche boundary in determining maximum velocity and run-out distance.

RÉSUMÉ. *Un modèle d'écoulement par fragments d'avalanches de neige sèche.* Des données d'observation sur les avalanches de plaques sèches obtenues pendant la période 1975–79 sous divers climats enneigés aboutissent aux conclusions suivantes: (1) la plus grande partie de la masse de l'avalanche typique étudiée était composée de fragments de plus de 5 cm de longueur, (2) des plans de cisaillements transversaux et longitudinaux se formaient pendant la période de décélération de l'avalanche dans la zone de dépôt, et (3) la hauteur de l'écoulement dépassait dans la plupart des cas celle de la plaque. On n'a pas trouvé de corrélation entre la distance d'arrêt et la pente du couloir ou de la zone de dépôt ou entre la distance d'arrêt et la hauteur de la plaque déclenchée.

Les données d'observation suggèrent que la meilleure description du mouvement de l'avalanche est celle d'un écoulement de fragments dans lequel les efforts de cisaillement en limite sont sensibles aux distributions des tailles des fragments et aux concentrations en volume des solides. Ces facteurs peuvent être plus importants que la rugosité du lit de l'avalanche pour la détermination de la vitesse maximum et de la distance d'arrêt.

ZUSAMMENFASSUNG. *Ein Modell des Bruchstückflusses für Trockenschneelawinen.* Feldbeobachtungen an trockenen Schneebrettlawinen, angestellt im Zeitraum von 1975 bis 1979 in verschiedenen Schneegebieten, führen zu folgenden Schlüssen: (1) Der Grossteil der Masse des untersuchten Lawinentyps bestand aus Bruchstücken mit Längen von mehr als 5 cm; (2) Quer- und Längsscherebenen bildeten sich während der Verzögerung in der Auslaufzone; (3) die Stromhöhe übertraf in den meisten Fällen die Bretthöhe. Zwischen der Reichweite und der Neigung der Bahn oder der Auslaufzone war keine Korrelation festzustellen, ebensowenig zwischen der Reichweite und der freigesetzten Bretthöhe.

Die Feldbeobachtungen lassen vermuten, dass sich die Lawinenbewegung am besten als Fluss von Bruchstücken beschreiben lässt, in der die randlichen Scherspannungen von der Grössenverteilung der Bruchstücke und der Konzentration an Festkörpern abhängt. Die Faktoren dürften für die Bestimmung der Höchstgeschwindigkeit und der Reichweite wichtiger sein als die Rauhigkeit der Lawinenbegrenzung.

INTRODUCTION

Previous avalanche-dynamics research (Voellmy, 1955; Sommerhalder, 1966; Salm, 1966; Shen and Roper, 1970; Mears, 1975, 1976, 1977; Leaf and Martinelli, 1977; Lang and others, 1978), assumes the avalanches behave as fluids in which particle sizes are small compared with flow dimensions and that the flow is incompressible. In such models fluid properties such as eddy and molecular viscosity act to resist avalanche acceleration from the beginning of motion in the starting zone through deceleration in the run-out zone. However, fluid models do not consider the internal structural changes that occur during motion.

The objective of the research presented in this paper is to discuss and identify the parameters that appear to be of greatest importance in determining the internal structure, boundary shear stresses, run-out distance, and, by inference, the velocity of dry-snow avalanches. The first part of this paper reports general observations and data from 45 moderate to large dry-snow avalanches studied during the four winters from 1975 through 1979. Data were collected from avalanches with large mean slab heights or long run-out distances and were obtained from the San Juan Mountains, the Elk Mountains, the Ten Mile Range, and the Front Range of Colorado, from the Wasatch Mountains of Utah, and from the Chugach Mountains of south-central Alaska. Thus the data are not biased toward any one particular snow climate or mountain region.

https://doi.org/10.3189/S0022143000010698 Published online by Cambridge University Press

The second part of the paper suggests how the most important features observed in the field can be explained analytically. The emphasis of the second part is to show which flow parameters appear to be most important in determining avalanche velocity and run-out distance, but it is recognized that a final predictive model based on the parameters discussed below requires collection of additional data.

Run-out distance

When an avalanche is modeled as an incompressible fluid, the velocity and run-out distance S increase with the thickness h of the released slab, the slope α of the track, and the run-out slope β. In this study four variables were obtained: S, α, β, and h. The slope parameters α and β and the thickness h were measured in the field and S was scaled from topographic maps or measured in the field. Avalanche velocity was measured in a few selected cases, but insufficient velocity data exist to be included in this analysis.

As defined in this study, the run-out zone begins where deposition of avalanche debris exceed entrainment of undisturbed snow into the flow. Thus within the run-out zone $\mathrm{d}M/\mathrm{d}L < 0$, where M is the avalanche mass and L is the distance traveled. The run-out distance S was measured from the beginning of this area of deposition and corresponded, for large dry-snow avalanches, to a slope of 15° to 20°.

The track corresponded to $15° \leqslant \alpha \leqslant 30°$, gradients upon which $\mathrm{d}M/\mathrm{d}L \approx 0$ and deposition of avalanche snow is approximately balanced by entrainment of new snow. Maximum velocity and maximum flowing mass both occur in the track. In several cases the mean track gradient exceeded 30° because of sections of steep rock outcrops in the track, but, because these steep areas do not collect sufficient quantities of snow, the condition $\mathrm{d}M/\mathrm{d}L = 0$ remained approximately true.

The starting zones correspond, approximately, to $\alpha > 30°$, slopes upon which $\mathrm{d}M/\mathrm{d}L > 0$ and avalanches accelerate and grow in mass (Fig. 1). Note that the conditions $\alpha > 30°$ and $\mathrm{d}M/\mathrm{d}L > 0$ may be satisfied at many locations adjacent to the avalanche track, particularly

Fig. 1. Striations on the avalanche running surface and linear depositional features parallel to the avalanche direction suggest basal sliding in the starting zone of this hard-slab avalanche. The mean slope angle in the photograph is 35°.

https://doi.org/10.3189/S0022143000010698 Published online by Cambridge University Press

when a relatively windless storm has deposited unstable slabs on steep slopes over large elevation differences and when the avalanche tends to release and entrain these unstable slabs (Fig. 2). The term dM/dL serves as an inertial effect that resists acceleration as the momentum of the snow at rest is increased as it is entrained into the moving avalanche.

Fig. 2. Snow entrained at the steep lateral boundaries of the avalanche track cause the avalanche mass to increase with distance traveled ($dM/dL > 0$). *Such entrainment is an inertial effect resisting avalanche acceleration during the beginning stages of motion.*

In Figure 3, S is plotted against h, α, and β for 29 dry-slab avalanches with clearly-defined run-out limits and run-out zones not terminated by an adverse (reversed-gradient) slope. There is no statistically significant variation of S with h, α, and β in the sample obtained. In general, the larger slab heights (in excess of 1.5 m) were associated with strongly-bonded, high-density wind slabs that fractured into large blocks (Fig. 4), while the longer run-out distances were associated with less thick soft slabs that fractured into smaller fragments (Fig. 5).

Composition, form, and distribution of debris in the run-out zone

Most of the debris mass of the run-out zone appears to consist of fragments derived from the released slab. The intermediate diameter d of these fragments ranges from approximately 2 to 150 cm. As a rough estimate, based on observations of the deposit surfaces and lateral boundaries and in a few cases from observations below the debris surface, at least 80 to 90% of the total avalanche mass within the typical dry-slab avalanche studied consisted of fragments larger than 5 cm in intermediate diameter. This length, defined as a characteristic fragment size d^*, tends to be much larger in hard-slab avalanches (20 to 30 cm), than in soft-slab avalanches (compare Figs 4, 5, and 6). If avalanches remained dry to the distal margin of the run-out zone, it was difficult to distinguish between individual fragments approximately 1 m or more below the debris surfaces. Deep within the debris, the slab fragments and fine-grained interstitial snow were compressed together to densities of 300 kg/m^3 to 530 kg/m^3, with the larger densities being associated with larger avalanches. In several of the cases

https://doi.org/10.3189/S0022143000010698 Published online by Cambridge University Press

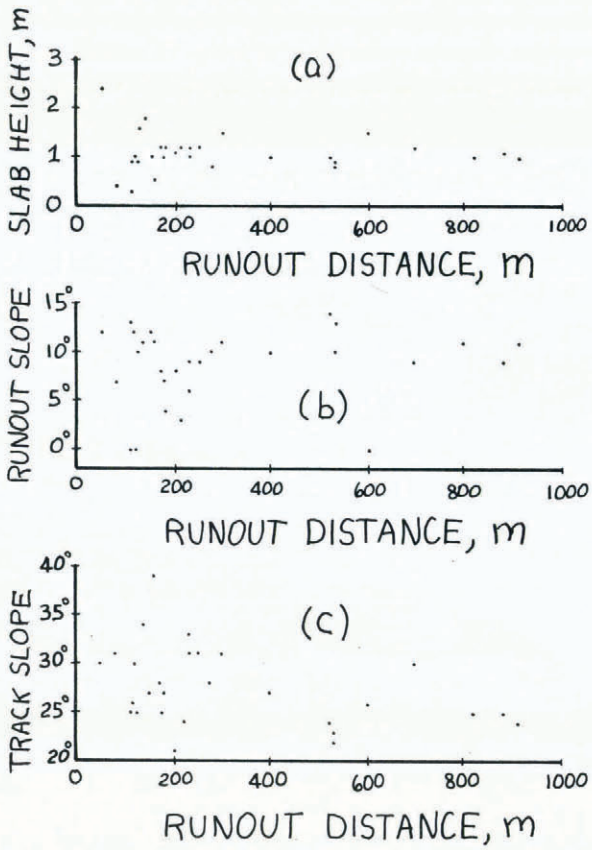

Fig. 3. These run-out-distance data were taken from dry-snow avalanches that did not encounter adverse (reversed-gradient) slopes in the run-out zone. The data include a wide range in slab density and cohesiveness. (a) Slab height is averaged over the crown length and measured perpendicular to the slope. (b) Run-out zones were assumed to begin on slopes of 15° to 20° where deposition of snow clearly exceeded entrainment. (c) Track gradients were measured over that portion of the path where $\mathrm{d}M/\mathrm{d}L \approx 0$, *corresponding to slopes of 15° to 30° in most cases. The steeper track gradients included in the data are associated with steep cliff areas in the track.*

studied large dry-slab avalanches flowed through damp snow in the lower track. Observations of such avalanches in motion suggest that some of the damp, finely-pulverized snow dispersed in the flow adheres to the flowing fragments causing the fragments to become more spherical with distance traveled. Because much of the fine-grained fraction of the flow adhered to the larger fragments, very little was left to cement the deposit at depth, thus individual fragments could be distinguished from one another within the deposits.

When the topography of the run-out zone consisted of relatively smooth, unconfined slopes, the debris was spread uniformly, decreasing gradually in thickness from a maximum of 2 to 4 m at the top of the run-out zone to less than 1 m near the distal margin. In general, fragment sizes decreased within a given deposit from a maximum characteristic size $d^\star$ near the top to some smaller $d^\star$ near the toe of the run-out zone. When different avalanche events were compared, S was always significantly longer for smaller $d^\star$ and shorter for larger $d^\star$ regardless of variation in α, β, or h. Thus S may be some empirical function of a size distribution in d. Insufficient data exist at the present time to suggest any unique statistical relationship between S and d.

https://doi.org/10.3189/S0022143000010698 Published online by Cambridge University Press

Fig. 4. Particle sizes at the distal margin of this hard-slab avalanche suggest that at this location at least 90% of the avalanche mass consisted of fragments with $d > 15$ cm, thus $d^* = 15$ cm. Approximately 100 m up-slope from this location (not shown), d^* was estimated as 30 to 40 cm. The fine-grained fraction of the flow was not transported beyond the distal margin of the fragments, or was of negligible mass.

Fig. 5. This thin deposit is located at the distal margin of a large dry-slab avalanche and is composed of small fragments admixed with fine particles. Larger fragments were deposited higher in the run-out zone.

https://doi.org/10.3189/S0022143000010698 Published online by Cambridge University Press

Fig. 6. Transverse and longitudinal shear planes in the run-out zone of this large dry-slab avalanche suggest that the avalanche mass deformed as a solid body during the final stages of deceleration. Surface ridges and furrows indicate that stresses were transmitted over distances of at least several meters. In this case $d^{\star} = 5$ cm, and the avalanche had fallen approximately 800 m vertically.

Fig. 7. Distinct longitudinal shear planes parallel with the flow occurred in this large dry-slab avalanche that encountered damp snow in the lower track. The reaggregated mass of fragments slid as a solid body for approximately 300 m on a 16° slope. The sliding mass consisted of fragments with $5 \text{ cm} \leqslant d \leqslant 40$ cm. The tension crack in the shear plane in the foreground shows that fragments were preserved inside the sliding mass.

https://doi.org/10.3189/S0022143000010698 Published online by Cambridge University Press

Transverse shear planes were observed in some debris when the depth exceeded 1 to 2 m, occurring during decelerating portions of the flow. However, they were not observed within the deposits of smaller fragments or at the distal margins of long run-out zones (Fig. 5).

In several cases in which fragments could be identified throughout the deposit depth, there was a strong tendency for larger fragments to be sorted toward the centers and upper surfaces of the deposits, away from the regions where the velocity gradients in the flowing mass would be largest.

Longitudinal shear planes were one of the most striking features of many avalanche deposits, including those formed as dry-snow avalanches flowed through damp snow in the lower track (Fig. 7), and those formed from avalanches that remained dry throughout the entire path (Fig. 8). These features demonstrate that differential sliding occurred in both damp and dry snow. The sliding bodies were clearly composed of reaggregated fragments of the slab in all cases studied, and were 3 to 15 m wide and 1 to 3 m deep. Sliding distances were as long as 150 m on a slope of 15° through dry snow, and up to 400 m on a slope of 16° through damp snow. The longer distances were associated with some channelization in the upper run-out zones, but shear planes also occurred within unconfined run-out zones.

Fig. 8. This longitudinal shear plane is parallel to the avalanche flow direction and is typical of shear planes observed in the run-out zones of dry-snow avalanches. Typical fragment sizes are visible but somewhat obscured by a thin deposit of fine-grained snow.

Flow height

Knowledge of the flow height h_f is of great importance in engineering design of avalanche defense structures. In the early Swiss work (Voellmy, 1955; Sommerhalder, 1966), it was assumed that $h_f = h$, allowing for changes in h_f due to slope changes, as in water flow in an open channel. In the field it is difficult to distinguish the lower layer of flowing and sliding snow thought to comprise most of the avalanche mass from a deeper, dispersed powder cloud, therefore indirect methods must be used to estimate flow height. Field observations of avalanche snow compressed against trees suggest that most of the avalanche mass is concentrated within a lower layer where $h \leqslant h_f \leqslant 4h$. It is assumed that most of the avalanche mass

https://doi.org/10.3189/S0022143000010698 Published online by Cambridge University Press

within this layer of thickness h_f consisted of slab fragments, as discussed above. This assumption is supported by avalanche impact measurements (Schaerer, 1973) in which distinct impact peaks were recorded, presumably due to fragment collisions with the pressure cell.

The larger ratios of h_f/h were associated with high-velocity soft-slab avalanches while the smaller ratios are associated with low-velocity hard-slab avalanches. Thus the mean free distance between fragments would tend to become longer and the mean bulk density of flow less in high-velocity avalanches comprised of small fragments. In some avalanches a small part of the mass was dispersed upward as a powder cloud to a height h_p, where $5h \leqslant h_p \leqslant 15h$, approximately. This fine-grained fraction of the flow probably traveled at high velocity and was of low mean bulk density, but nevertheless, had energy sufficient to damage trees in the path. Figure 9 illustrates an example where avalanche snow was compressed against a tree in the upper run-out zone of a large soft-slab avalanche. In this case $h_f = 2$ m and is determined by the height of compressed snow against the tree trunk, but, although no snow was compressed above h_f, limbs were broken to a height of approximately 10 m. Within this 10 m layer, the flow must have been of low bulk density and probably produced fluid-dynamic forces such as a gust of wind.

The field estimates of h_f were considered reliable only if ten or more measurements were made within smooth reaches of the path, and if the standard error of the mean was less than $0.1h_f$.

Fig. 9. Compressed snow on this tree in the upper run-out zone indicates that $h_f = 2$ m. Broken limbs on the tree indicate that the powder avalanche flow height $h_p = 10$ m.

https://doi.org/10.3189/S0022143000010698 Published online by Cambridge University Press

The data obtained strongly suggest that, for engineering design purposes, it should be assumed that the fractured slab is dispersed upward to some height larger than h during flow. The ratio h_f/h depends on the characteristics fragment size d^*, and probably on flow velocity U, both of which appear to depend more on initial slab cohesiveness than on slab height.

Parameters controling avalanche velocity and acceleration

The observations reported above suggest that dry-slab avalanches consist of a cascade of slab fragments admixed with fine-grained snow in suspension. Most of the mass within the avalanches studied consisted of fragments too large to be suspended by air turbulence according to the criteria described by Shōda (1966), therefore, the upward dilation of particles required for flow to be possible must be maintained by collisions between the fragments. The internal energy loss in the fragment flow and the resulting boundary shear may be affected by the size and density distributions of the fragments and by the mean free distance between them because these factors help control collision frequency.

The gravitational driving stress τ_g per unit of avalanche boundary is written:

$$\tau_g = \rho g h \sin \alpha, \tag{1}$$

where ρ is the mean bulk density over the flow height h, g is the gravitational acceleration, and α is the slope angle.

The resisting stress τ_s is a function of avalanche velocity and internal structure. Bagnold (1954) derived an expression for shear within a rapidly sheared dispersion of small parafin spheres. When inertial effects dominate over the viscous effects of the interstitial fluid, as probably would be the case in most avalanches, the general form of this expression is written:

$$\tau_s' = f(\phi)\, f(C_s)\, \sigma d^2 (dU/dy)^2, \tag{2}$$

where τ_s' is the shear stress at any point in the fragment flow, ϕ is a dimensionless coefficient that depends upon collision condition, d is particle diameter, C_s is solids concentration, σ is particle density, and dU/dy is the velocity gradient normal to the flow boundary. Bagnold's experimentally determined values for boundary shear cannot be used directly to determine avalanche boundary shear because, within an avalanche σ and d are not uniform, C_s varies with height, and flow dimensions are much larger than those of Bagold's experiments. However, he did find τ_s' to be proportional to d^2 and to increase very rapidly with C_s. For example, at constant $\sigma d^2 (dU/dy)^2$ he found τ_s' to increase by more than a factor of 10 as C_s increased from 0.30 to 0.60. This is the same range of C_s as is to be expected in an avalanche. If the same relationships hold true in an avalanche, then hard slabs with characteristically larger d would experience larger τ_s, reach lesser velocities, and travel shorter distances than soft-slab avalanches with smaller d. This is consistent with field observations. Furthermore, because an avalanche is characterized by a distribution of d values, the smaller fragments would be subjected to lesser stress, would attain higher velocities, and would travel farther. This offers one explanation for the longitudinal sorting observed.

If the form of Equation (2) is correct, then boundary shear within a fragment-flow may be written:

$$\tau_s = D_s C_s \sigma U^2, \tag{3}$$

where U is the mean velocity over the flow cross-section and D_s is a "solid drag" coefficient assumed to include the effects of fluid-dynamic drag and mass change. It is important to note that:

$$D_s = f(C_s, d), \tag{4}$$

and

$$C_s = f(U). \tag{5}$$

Because it is assumed that inertial effects dominate, Equation (3) appears to give τ_s proportional to U^2. However, during acceleration the boundary stress may in fact *decrease* with U

https://doi.org/10.3189/S0022143000010698 Published online by Cambridge University Press

because C_s decreases with U as the flow height increases. D_s as determined in the experiments of Bagnold (1954), appears to be strongly dependent upon C_s. In the field it was common to find that soft-slab avalanches achieved greater flow depths than hard-slab avalanches even though the soft slabs were, in general much thinner than the hard slabs.

A positive feed-back mechanism may occur during acceleration as D_s decreases with increasing U. This feed-back mechanism would be damped due to the inertial effects of new snow entrainment and air resistance (both proportional to U^2 and considered in the D_s term), but computations suggest that air resistance will probably not be important in an avalanche with flow height less than 5 m until U exceeds 30 m/s. New snow entrainment is probably not important as maximum velocity is approached because the mass of new snow entrained into the flow is probably a small proportion of total mass.

Similarly, a negative feed-back mechanism may operate during deceleration. As U decreases, C_s and D_s would increase, thereby increasing the τ_s term and causing further deceleration. This offers one explanation for the observation that dry-snow avalanches tend to decelerate rapidly in the run-out zone. The shear planes described above may also be explained because at small U the fragment flow condenses and interlocks. This rapidly increases τ_s and may cause slip at the boundaries.

Interestingly, Schaerer ([1975]) also reports an increase in frictional resistance with decreasing U. He suggested the friction increase was due to an increase in the sliding friction coefficient μ (discussed below), but this effect can also be explained through the negative feed-back mechanism described above.

When Equations (1) and (3) are equated and it is assumed that mass entrainment is negligible at maximum velocity, then

$$U^2 = (g/D_s)\, h \sin \alpha, \tag{6}$$

where $\rho = C_s\sigma$. The largest avalanches approach 100 m/s (Mellor, 1968) thus the factor gh/D_s approaches 2×10^4 m^2/s^2. Assuming h equals 10 m for the largest dry-slab avalanches (disregarding the very deep, diffuse powder cloud), and g equals 10 m/s^2, then D_s may be as small as 5×10^{-3}. This should be considered a limiting value rarely achieved in Nature because of the effects of air resistance at high velocities.

In Voellmy's two-component model, at terminal velocity

$$\tau_g = \tau + \tau_f, \tag{7}$$

where τ is boundary shear due to sliding and τ_f is boundary shear due to fluid turbulence. Note that τ_f is included in the τ_s term discussed above, but does not become important until high velocity is attained.

If

$$\tau = \mu \rho g h \cos \alpha, \tag{8}$$

and

$$\tau_f = D_f \rho U^2, \tag{9}$$

then

$$\rho g h \sin \alpha = \mu \rho g h \cos \alpha + D_f \rho U^2, \tag{10}$$

where μ is a coefficient of sliding friction and D_f is a fluid drag coefficient which is highly dependent on surface roughness. Solution of Equation (10) for U^2 gives Voellmy's well-known equation for maximum velocity

$$U^2 = \xi h(\sin \alpha - \mu \cos \alpha), \tag{11}$$

where ξ, the "turbulent friction" coefficient, is substituted for g/D_f. The parameter D_f depends only on surface roughness; released snow type or degree of fragmentation are not considered.

https://doi.org/10.3189/S0022143000010698 Published online by Cambridge University Press

A non-zero friction coefficient μ is necessary in Equation (11) because, when μ equals zero steady flow may be maintained whenever α is greater than zero.

Field calibration of Equation (11) is not possible because, even if U, α, and h are measured: the observed U may result from an infinite number of μ, ξ pairs. However, using the same approach, a unique value of D_s may be computed for Equation (6). Field studies may allow calibration of D_s with flow height and observed fragment-size distributions, parameters which may eventually be correlated with slab conditions expected at the times of large avalanche releases.

Acknowledgements

Field data discussed in the first part of this paper were collected by the author while employed as a research consultant to the United States Forest Service, Rocky Mountain Forest and Range Experiment Station. Assistance in the collection of these data was provided by Don Bachman, Doug Fesler, Henry Santeford, Nancy Simmerman, and Doug Wolfe.

Discussions about the physics of avalanche motion with Don Bachman, M. Martinelli, Jr, David McClung, and Ron Perla helped me to think a little more clearly. I also wish to thank a *Journal of Glaciology* referee whose name is unknown to me.

REFERENCES

Bagnold, R. A. 1954. Experiments on a gravity-free dispersion of large solid spheres in a Newtonian fluid under shear. *Proceedings of the Royal Society of London*, Ser. A, Vol. 225, No. 1160, p. 49–63.

Daugherty, R. L., *and* Franzini, J. B. 1965. *Fluid mechanics with engineering application.* New York, McGraw-Hill Book Co., Inc.

Lang, T. E., *and others.* 1978. Numerical hydrodynamic simulation of snow avalanche flow, by T. E. Lang, K. L. Dawson, and M. Martinelli, Jr. *U.S. Dept. of Agriculture. Forest Service. Research Paper* RM-205.

Leaf, C. F., *and* Martinelli, M., *jr.* 1977. Avalanche dynamics: engineering applications for land use planning. *U.S. Dept. of Atriculture. Forest Service. Research Paper* RM-183.

Mears, A. I. 1975. Dynamics of dense-snow avalanches interpreted from broken trees. *Geology*, Vol. 3, No. 9, p. 521–23.

Mears, A. I. 1976. Guidelines and methods for detailed snow avalanche hazard investigations in Colorado. *Colorado. Geological Survey. Bulletin* 38.

Mears, A. I. 1977. Snow avalanche hazard identification and delineation. *Colorado. Geological Survey. Special Publication* 8, p. 21–26.

Mellor, M. 1968. Avalanches. U.S. Cold Regions Research and Engineering Laboratory. *Cold regions science and engineering.* Hanover, N.H., Pt. III, Sect. A3d.

Salm, B. 1966. Contribution to avalanche dynamics. *Union de Géodésie et Géophysique Internationale. Association Internationale d'Hydrologie Scientifique. Commission pour la Neige et la Glace. Division Neige Saisonnière et Avalanches. Symposium international sur les aspects scientifiques des avalanches de neige, 5–10 avril 1965, Davos, Suisse*, p. 199–214. (Publication No. 69 de l'Association Internationale d'Hydrologie Scientifique.)

Savage, S. B. 1979. Gravity flow of cohesionless granular materials in chutes and channels. *Journal of Fluid Mechanics*, Vol. 92, Pt. 1, p. 53–96.

Schaerer, P. A. 1973. Observations of avalanche impact pressures. *U.S. Dept. of Agriculture. Forest Service. General Technical Report* RM-3, p. 51–54.

Schaerer, P. A. [1975.] Friction coefficients and speed of flowing avalanches. [*Union Géodésique et Géophysique Internationale. Association Internationale des Sciences Hydrologiques. Commission des Neiges et Glaces.*] *Symposium. Mécanique de la neige. Actes du colloque de Grindelwald, avril 1974*, p. 425–32. (IAHS–AISH Publication No. 114.)

Shen, H. W., *and* Roper, A. T. 1970. Dynamics of snow avalanches (with estimation for force on a bridge). *Bulletin of the International Association of Scientific Hydrology*, Vol. 15, No. 1, p. 7–26.

Shōda, M. 1966. An experimental study on dynamics of avalanches snow. *Union de Géodésie et Géophysique Internationale. Association Internationale d'Hydrologie Scientifique. Commission pour la Neige et la Glace. Division Neige Saisonnière et Avalanches. Symposium international sur les aspects scientifiques des avalanches de neige, 5–10 avril 1965, Davos, Suisse*, p. 215–29d. (Publication No. 69 de l'Association Internationale d'Hydrologie Scientifique.)

Sommerhalder, E. 1966. Lawinenkräfte und Objektschutz. *Schnee und Lawinen in den Schweizeralpen. Winterbericht des Eidg. Institutes für Schnee- und Lawinenforschung*, Nr. 29, Winter 1964/65, p. 134–41. [English translation: Avalanche forces and the protection of objects. *U.S. Dept. of Agriculture. Forest Service. Alta Avalanche Study Center Translation* No. 6, 1967. Revised and supplemented January 1978.]

Voellmy, A. 1955. Über die Zerstörungskraft von Lawinen. *Schweizerische Bauzeitung*, Jahrg. 73, Ht. 12, p. 159–62; Ht. 15, p. 212–17; Ht. 17, p. 246–49; Ht. 19, p. 280–85. [English translation: On the destructive force of avalanches. *U.S. Dept. of Agriculture. Forest Service. Alta Avalanche Study Center Translation* No. 2, 1964.]

https://doi.org/10.3189/S0022143000010698 Published online by Cambridge University Press